Journal of Hazardous Materials 198 (2011) 1–6

Contents lists available at SciVerse ScienceDirect

Journal of Hazardous Materials

journal homepage: www.elsevier.com/locate/jhazmat

Novel $KMnO_4$-modified iron oxide for effective arsenite removal

Yao-Hui Huang[a,b,*], Yu-Jen Shih[a], Fu-Ji Cheng[a]

[a] Department of Chemical Engineering, National Chen-Kung University, Tainan, Taiwan
[b] Sustainable Environment Research Center, National Cheng Kung University, Tainan, Taiwan

ARTICLE INFO

Article history:
Received 8 July 2011
Received in revised form
30 September 2011
Accepted 1 October 2011
Available online 20 October 2011

Keywords:
Fluidized bed reactor
Goethite
Oxidation
Immobilization
Adsorbent

ABSTRACT

This work demonstrates the synthesis of a novel $KMnO_4$-modified form of iron oxide, MnBT-4, using a fluidized bed reactor (FBR) for the adsorptive removal of arsenic (III)/(V). Characterization by XRD, BET, and SEM indicated that the BT-4 support was poorly crystallized goethite (α-FeOOH) with a specific surface area of 229 $m^2\ g^{-1}$. In FBR experiments of synthesizing MnBT-4, the Fe and Mn salts were found to have an optimal dosage ratio of less than 4, which maximized the $KMnO_4$ immobilization efficiency. The immobilized Mn compounds on MnBT-4 underwent an additional oxidation step of As (III), promoting arsenic adsorption. When applied MnBT-4 for As (III) removal from solution, the sorption isotherm was accurately fitted with Langmuir and Freundlich models, while the maximum adsorption capacity of 27.4 mg g^{-1} exceeded those of other adsorbents in the literature. Batch experimental results revealed that both raw BT-4 and MnBT-4 could take up a large amount of As (V). However, the MnBT-4 provided a substantially higher As (III) removal efficiency than BT-4.

1. Introduction

Little arsenic is present in the natural environment but it can be found everywhere because it dissolves out of soil and weathered rock. However, human civilization, including agricultural, traditional and Hi-tech industry, has produced a large amount of wastewater markedly increasing the arsenic content in water. The long-term uptake of bio-accumulated arsenic in water and food is harmful to the vital organs, posing a serious health risk to humans. The World Health Organization (WHO) in 1993 has set a guideline limit of 10 μg L^{-1} in drinking water. In natural water, arsenic is typically present in inorganic forms, of which As (III) and As (V) dominate. Arsenite [As (III)] is much more toxic, soluble and mobile than arsenate [As (V)]. Besides, in the normal pH range (pH 6–8), As (III) preferentially exists in an uncharged form ($H_3AsO_3{}^0$), which is the dominant species in groundwater [1], and is much more difficult to remove by conventional physicochemical methods than is As (V) [2].

Several approaches, including adsorption [3], ion-exchange [4], precipitation [5], coagulation [6,7], filtration [8,9], and reverse osmosis [10], have been developed for arsenic removal from water. Among these, adsorption is considered to be easy and cost-efficient. Much research on appropriate adsorbents for removing arsenic has recently been conducted. Iron oxides are the most popular adsorbents owing to their high affinity for inorganic arsenic species [11–15]. However, As (III) adsorption is generally less effective than the As (V) adsorption. To overcome this difficulty, the use of a binary oxide, comprising manganese oxide as an oxidant and iron oxide as an adsorbent, has been proposed [16]. Manganese oxides have been extensively studied as oxidizing agents specifically for oxidation of As (III), while Mn (IV) has been reduced to Mn (III) and to Mn (II), as in reactions (1)–(3) [17–19].

$$H_3AsO_3 + MnO_2 + 2H^+ \leftrightarrow H_3AsO_4 + Mn^{2+} + H_2O \quad (1)$$

$$H_3AsO_3 + 2MnO_2 \leftrightarrow 2MnOOH + H_3AsO_4 \quad (2)$$

$$H_3AsO_3 + 2MnOOH + 2H^+ \leftrightarrow HAsO_4{}^{2-} + 2Mn^{2+} + 3H_2O \quad (3)$$

However, manganese oxide is not a suitable adsorbent for removing arsenic [20]. Hence Zhang et al. [21] investigated a novel Fe–Mn binary oxide as adsorbent for efficiently removing arsenic. When the redox system is maintained at pH 7–8, the dissolved ferrous and permanganate salts coprecipitated as the ferrous–manganese base hydroxide:

$$3Fe^{2+} + MnO_4{}^- + 4OH^- + 3H_2O \rightarrow 3Fe(OH)_{3(s)} + MnO_{2(s)} + H^+ \quad (4)$$

The pre-oxidation of As (III) by the MnO_2 fraction apparently promotes the removal of total arsenic from water by the iron oxide fraction.

To the best of the authors' knowledge, ease of recycling and reuse are keys to the selection of a candidate adsorbent. Although it has a high capacity to uptake and remove As (III), the nano- to micro-meter-scaled precipitates of Fe–Mn binary oxide may not be

* Corresponding author at: Department of Chemical Engineering, National Chen-Kung University, Tainan, Taiwan. Tel.: +886 6 275 7575x62636; fax: +886 6 234 4496.
E-mail address: yhhuang@mail.ncku.edu.tw (Y.-H. Huang).

0304-3894/$ – see front matter © 2011 Elsevier B.V. All rights reserved.
doi:10.1016/j.jhazmat.2011.10.010

effective for practical arsenic treatment. Hence, this investigation applies a masking concept, in which the Mn species is trapped onto the surface of a millimeter-scale BT-4 substrate in a fluidized bed reactor (FBR). When the hydraulics of FBR are properly controlled, BT-4 as a support can recovery the products of the redox reaction between ferrous and permanganate salts in solution. BT-4 is a waste iron oxide obtained from the real fluidized bed-Fenton (FBR-Fenton) instruments [22]. Since the FBR-Fenton process performed the long-term wastewater treatment, the derived iron hydroxide has been homogeneously crystallized, and the crystals accumulated as particles of half to several millimeters in the reactor. Hence, the use of a BT-4 support can increase the cost-efficiency and ease of separation and disposal for the synthesis of the adsorbent, and further for arsenic removal.

Our previous studies have explored the capacity of BT waste iron oxide as an excellent adsorbent for removing F^-, PO_4^{3-}, Cu^{2+}, and Pb^{2+} because it has a high surface area and porosity [22–25]. Based on the concept of synthesizing Mn–Fe binary oxide in the literature [16], a fluidized bed reactor was utilized herein to perform the simultaneous co-precipitation and immobilization of Mn–Fe oxides on BT-4 iron oxide. The extent of immobilization of Mn on BT-4 was examined as a function of reaction time was by varying the initial Fe (II)/$KMnO_4$ ratio in solution. The MnBT-4 adsorbents that were formed by treating BT-4 with Mn were therefore used to explore the adsorption capacity of As (III). In addition, the efficiencies of BT-4 with and without Mn immobilization in the adsorptive removal of As (III) and (V) were compared.

2. Materials and methods

2.1. Materials

All chemicals were of analytical grade and used without purification. The As (III) and As (V) stock solutions were prepared using $NaAsO_2$ and $NaHAsO_4{\cdot}7H_2O$, respectively, which were purchased from KANTO CHAMICAL CO., INC. $FeCl_2$ and $KMnO_4$ were supplied by J.T. BAKER. All solution samples that were used in the FBR process and the adsorption experiments were prepared using deionized water (conductivity >18.3 MΩ) that had been purified using a laboratory-grade RO-ultrapure water system.

A BT-4 support was obtained from a real FBR-Fenton instrument which was used to treat tannery effluent wastewater. The micro morphology and the surface composition were observed using a scanning electron microscope (SEM, EOL JSM-6700F) and an energy dispersive spectrometer (EDS) (Oxford INCA-400). Crystallization was measured using X-ray diffraction (XRD), a counter diffractometer (Rigaku RX III) with Cu Kα radiation. The Brunauer–Emmett–Teller (BET) surface area ($m^2\,g^{-1}$), micro-pore area ($m^2\,g^{-1}$), external surface area ($m^2\,g^{-1}$), total pore volume ($cm^3\,g^{-1}$), and adsorption average pore diameter (Å) were measured using a surface area/porosity analyzer (Micromeritics ASAP 2010).

2.2. Synthesis of Mn-immobilized BT-4 (MnBT-4)

Fig. 1 presents the laboratory scale fluidized bed reactor (FBR) that was used to synthesize the MnBT-4 adsorbent. The FBR is a glass column with an internal diameter of 2 cm. The total height and batch volume are 80 cm and 550 mL, respectively. Firstly, 450 mL of deionized water was injected; BT-4 particles were loaded in the FBR, and the bed expansion was maintained at 50% by controlling the upstream flow rate. The pH of the solution that circulated in the FBR was kept at 3 by adding NaOH and HCl. Pre-conditioned salt solutions at known concentrations ($FeCl_2$ = 50 mL, $KMnO_4$ = 50 mL) were then fed into FBR to carry out the reaction. The final recovered

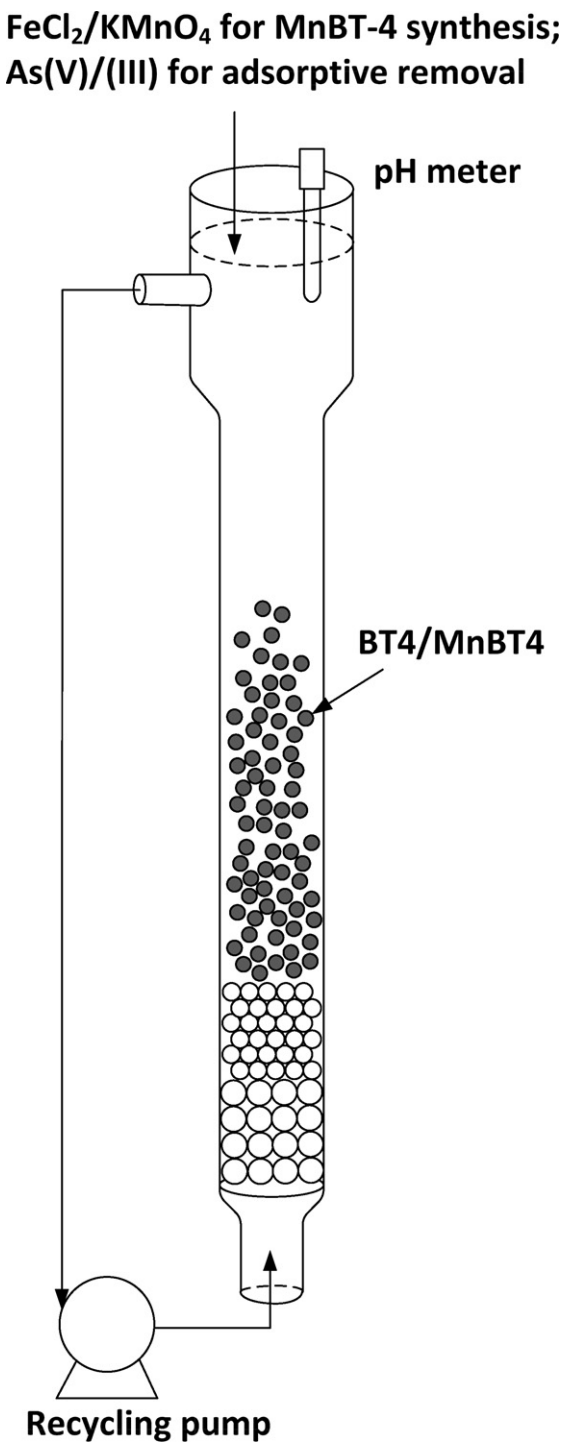

Fig. 1. Schematic fluidized bed reactor (FBR) for synthesizing MnBT-4 and arsenic adsorption experiments.

MnBT-4 sample was dried at 105 °C for 4 h and stored in a desiccator for subsequent use. Throughout the reaction period of 6 h, the residual Mn in the supernatants that were sampled from the effluent at fixed time intervals was analyzed using an atomic analysis spectrometer (AAS, SensAA Dual).

2.3. Batch As (III)/(V) adsorption experiments

The arsenic adsorption experiments were also conducted in an FBR system. After the BT-4/MnBT-4 adsorbents (2.5 g) that were

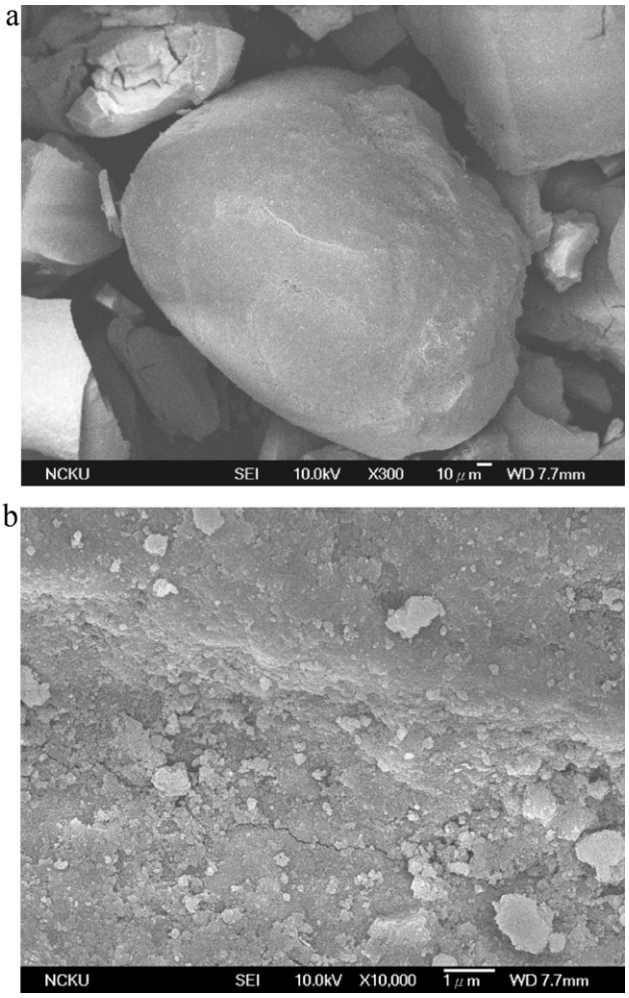

Fig. 2. Scanning electron microscopic (SEM) observation of BT-4 with magnitude (a) 300× and (b) 10,000×.

loaded in the FBR were fluidized using 500 mL deionized water, the pre-conditioned As (III)/(V) solution (50 mL) was injected to perform the adsorption experiment. Throughout the reaction period of 24 h, the solution pH was initially maintained at 3 by adding HCl and NaOH periodically. The As (III) adsorption isotherm for MnBT-4 was determined in a 500 ml glass vessel, with initial arsenic concentrations from 70 to 270 ppm. The extracted samples were filtered through a 0.45 μm membrane and the As concentrations of the solution were analyzed by an inductively coupled plasma-optical emission spectrometer (ICP-OES, ULTIMA 2000, HORIDA).

3. Results and discussion

3.1. Characterization of BT-4 iron oxide

Fig. 2 displays an SEM micrograph of BT-4 iron oxide in the form of millimeter-scale and rounded granular grains. Under higher magnification, the morphology is observed to be rough and the irregular surface of BT-4 exhibits locally aggregated hard nano-sized crystallites. The high specific surface area of 229 $m^2\,g^{-1}$ of BT-4 agrees in Table 1 agrees with SEM observations (Fig. 2). The many adsorption sites, bulk density of 1.56 and true density of 2.38 $g\,cm^{-1}$ accompany a granular size of 0.25–1 mm. These properties suggest that BT-4 is formed from fine iron hydroxide sludge, dewatering and compacting into hard aggregates. The XRD pattern in Fig. 3 reveals that BT-4 is goethite, as determined using the

Table 1
Characterization of BT-4.

Properties	Value
Average particle size, mm	0.25–1
Total iron content, mg g^{-1}	620
Apparent density, g cm^{-3}	1.43
True density, g cm^{-3}	2.41
BET specific surface area, $m^2\,g^{-1}$	229
Pore volume, $cm^3\,g^{-1}$	0.25

JCPDS diffraction standard, α-FeOOH phase. Moreover, the broadened peaks and noisy background reveal that the crystallinity of BT-4 is low.

3.2. $KMnO_4$-modified BT-4, MnBT-4

MnBT-4 was prepared by immobilizing the production of the redox reaction between potassium permanganate ($KMnO_4$) and iron chloride ($FeCl_2$) using BT-4 (40 g) as a support in an FRB. To avoid the precipitation of ferrous hydroxide and oxidation, the initial pH in FBR was fixed at 3. The initial concentration of potassium permanganate was conditioned to a fixed value ($[MnO_4^-]$ = 35 ppm), and the Fe (II) was adjusted to have the molar ratio (Fe/Mn ratio) to be 0, 1, 2, 4, and 6, respectively. The results in Fig. 4 demonstrate that the Fe/Mn ratio markedly affected the removal of Mn from solution. When the ratio was 1, the concentration of Mn was lower than 3 ppm after 6 h, indicating that 90% of Mn had been removed. However, the Mn removal efficiency declined as the Fe/Mn ratio increased, and an overdose of Fe (II) may affect the extent of Mn immobilization on BT-4. The change in Mn concentration in solution can be explained as follows. The reduction of permanganate by ferrous ions proceeded in two stages [26,27]; initially, the ferrous ions reduced Mn^{7+} to Mn^{4+}, and co-precipitates FeOOH and MnO_2 were immobilized by the BT-4 iron oxide:

$$3Fe^{2+} + MnO_4^- + 4H_2O \rightarrow FeOOH_{(s)\text{-BT-4}} + MnO_{2(s)\text{-BT-4}} + 5H^+ \quad (5)$$

Nevertheless, the ferrous ions might further reduce Mn^{4+} to Mn^{2+}:

$$2Fe^{2+} + MnO_{2(s)} + 4H_2O \rightarrow 2FeOOH_{(s)\text{-BT-4}} + Mn^{2+} + 2H^+ \quad (6)$$

Accordingly, the manganese oxides on BT-4 would reacted with a sufficient dose of free Fe (II), especially when the Fe/Mn ratio exceeded 2, and dissolved with the release of Mn^{2+} into solution. Therefore, excess Fe (II) relative to $KMnO_4$ retarded the formation of MnBT-4.

Notably, Mn immobilization occurred in the absence of ferrous ions (Fe/Mn ratio = 0), indicating that BT-4 iron oxide also served as

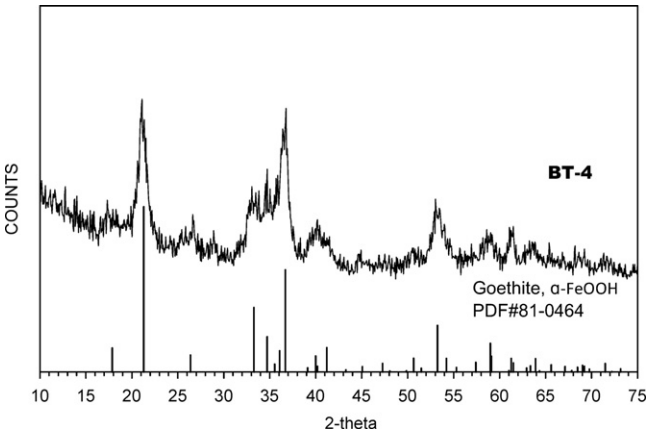

Fig. 3. X-ray diffraction (XRD) pattern of raw BT-4.

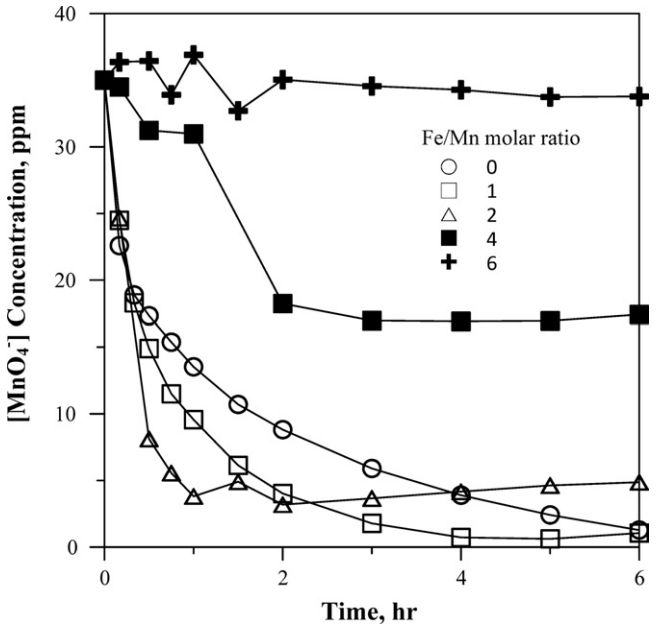

Fig. 4. Effect of Fe (II)/$KMnO_4$ ratio on Mn removal from the solution (initial $[MnO_4^-]$ = 35 ppm, BT-4 = 40 g).

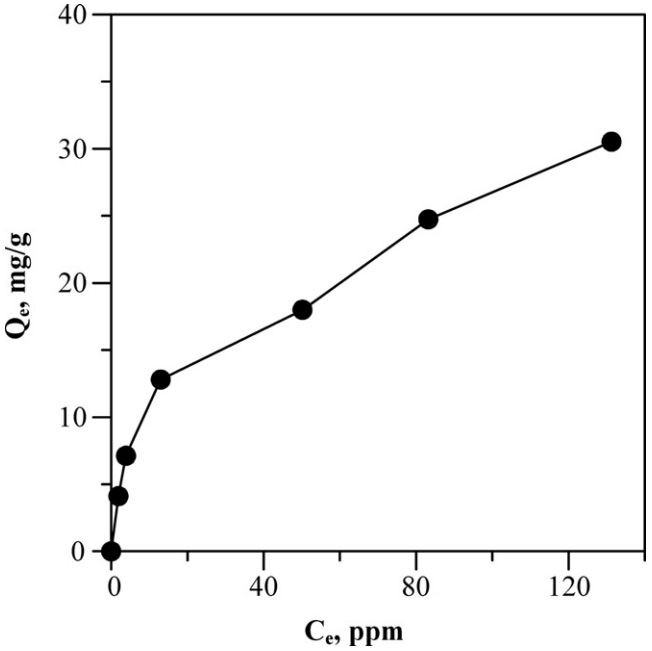

Fig. 6. Adsorption isotherm for As (III) by MnBT-4. (MnBT-4 = 2.5 g, pH = 3.)

a reductant of $KMnO_4$. Since Fe (II) was the catalyst of the generation of hydroxyl radicals during the formation of BT-4 in the Fenton process, the residual reactant $FeSO_4$ probably accumulated on BT-4, as evidenced by the trace amount of sulfate compound that was detected by the EDS analysis of the series of BT adsorbents in the authors' earlier investigation [25].

Since $KMnO_4$ was reduced by BT-4 alone, the effect of initial Mn concentration on the amount of prepared MnBT-4 without the addition of ferrous ions was further evaluated using the FBR system. A 40 g mass of BT-4 was reacted with various doses of $KMnO_4$ ($[MnO_4^-]$ = 35, 70, 175 and 350 ppm), while the initial pH was fixed at approximately 3. Fig. 5 reveals that the amount of immobilized Mn increased with initial $KMnO_4$ concentration. However, the immobilization efficiency was not proportional to the $KMnO_4$ dose. After the reaction had proceeded for 24 h, the amounts of residual

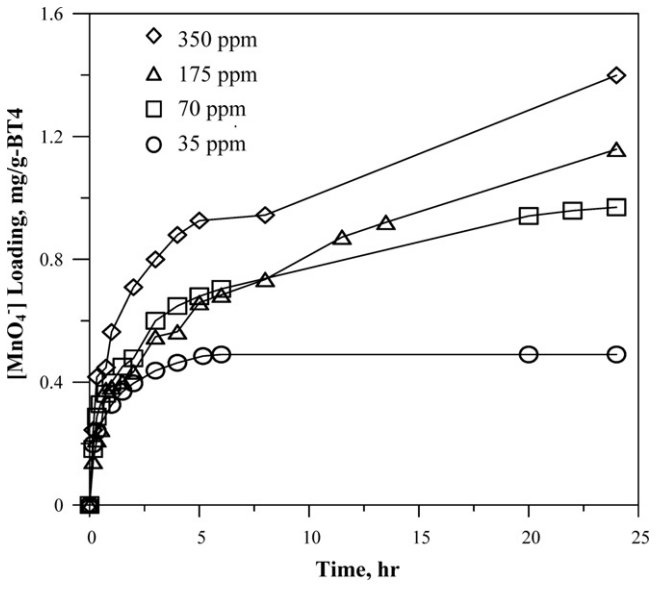

Fig. 5. Effect of initial $KMnO_4$ concentration ($[MnO_4^-]$ = 35, 75, 175 and 350 ppm) on the Mn loaded onto BT4. (BT-4 = 40 g.)

$[MnO_4^-]$ in solution were 0.2, 0.71, 82.4 and 255 ppm, and the calculated amounts of $[MnO_4^-]$ loaded onto per gram of BT-4 were 0.48, 0.94, 1.24 and 1.43 mg, respectively. The BT-4 sample that was treated with an initial $[MnO_4^-]$ of 175 ppm was selected as the MnBT-4 adsorbent in subsequent arsenic adsorption experiments.

3.3. Adsorptive removal of arsenic using MnBT-4

The capacity of the MnBT-4 adsorbent to adsorb As (III) was evaluated from the adsorption isotherms that are plotted in Fig. 6. The Langmuir and Freundlich models were utilized to identify the adsorption isotherm data as follows, where Q is the amount adsorbed at equilibrium (mg g^{-1}), and C_e is the equilibrium arsenic concentration (ppm):

$$\text{Freundlich model}: \quad Q = K_F C_e^{1/n} \tag{7}$$

$$\text{Langmuir model}: \quad Q = \frac{K_L Q_m C_e}{1 + K_L C_e} \tag{8}$$

Both models can be modified by linear regression:

$$\text{Freundlich model}: \quad \ln Q_e = \ln K_F + \frac{1}{n} \ln C_e \tag{9}$$

$$\text{Langmuir model}: \quad \frac{C_e}{Q_e} = \frac{1}{Q_m K_L} + \frac{C_e}{Q_m} \tag{10}$$

As shown in Fig. 7, the high regression coefficients ($R^2 > 0.95$) suggested that the As (III) adsorption isotherms were closely fitted using both models. Table 2 presents the isotherm parameters that were determined from the regression of the experimental data. K_F and n are related to adsorption capacity and intensity of the sorption, respectively, while K_L denotes the affinity of binding sites. At an n of one to ten, the Freundlich model indicates

Table 2
Langmuir and Freundlich isotherm parameters for As (III) adsorption on MnBT-4 adsorbent.

Langmuir model			Freundlich model		
Q_m, mg g^{-1}	K_L, L mg^{-1}	R^2	K_F, L mg^{-1}	n	R^2
27.4	0.066	0.957	4.41	2.62	0.9786

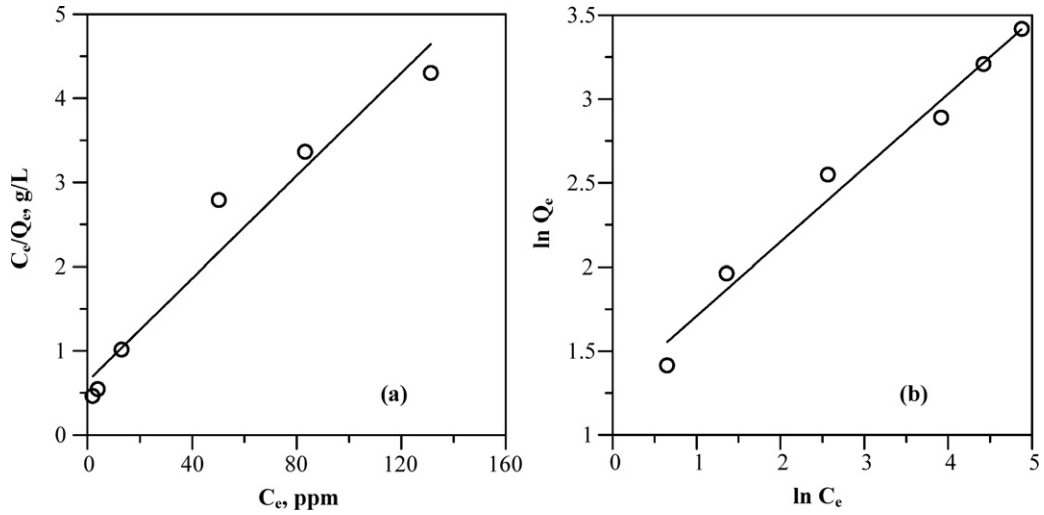

Fig. 7. The As (III) adsorption isotherm of MnBT-4 fitted with (a) Langmuir, and (b) Freundlich models.

Table 3
Summary of adsorption capacity values of As (III) on different adsorbent materials in recent literatures and present study.

Adsorbent	As (III) concentration	Surface area, $m^2\ g^{-1}$/particle size	Capacity, $mg\ g^{-1}$	Ref.
Ferro-compounds				
Zero-valent iron	50 ppm	3/8–50 mesh	7.5	[28]
Mn–Fe hydroxide	10 ppm	101/100 nm	4.58	[29]
Fe–Mn binary oxide	0.1 mM	265/26 μm	120	[21]
Iron oxide, Fe_2O_3	1 ppm	< 100 nm	1.94	[30]
Hematite	0.1 ppm	50/30–350 nm	2.1	[31]
Schwertmannite	1 mM	200/250 nm	9.75	[32]
MnBT-4	70 ppm	229/0.25–1 mm	27.4	Present study
Oxides				
Laterite	5 ppm	0.3–0.6 mm	0.2	[33]
Modified alumina	20 ppm	200/1–10 μm	10	[34]
LDHs	2 mM	1–10 μm	30	[35]
Cupric oxide	100 ppm	85/12–18 nm	26.9	[36]
Minerals				
Mica	10 ppm	10/2–50 μm	<0.5	[37]
Clay aggregate	0.15 ppm	<2 μm	<0.05	[38]

favorable adsorption. The n value calculated in this study, 2.62, implies that MnBT-4 is well suitable for arsenic adsorption. The maximum adsorption capacity, Q_m, that was estimated using the Langmuir model is 27.4 $mg\ g^{-1}$. MnBT-4 has a higher adsorption capacity than recently identified adsorbents for As (III) removal, including ferro-compounds, oxides, and clay minerals, as reviewed in Table 3. However, these adsorbents in the literature have a common feature: a higher specific surface area is normally associated with smaller particles on the nano- or micro-scale. This fact is a major shortcoming, which may be responsible for secondary pollution when such an adsorbent is used to treat real wastewater. By contrast, not only the porosity structure of BT4 could provide high specific surface area, but also the ease of free settling of hard aggregates makes BT-4 act as a more versatile adsorbent for practical treatments to remove arsenic.

Fig. 8 compares the As (III)/(V) adsorption efficiencies of BT-4 and MnBT-4 adsorbents. Clearly, both BT-4 and MnBT-4 adsorbents removed more than 95% of As (V) in 24 h, verifying that the iron oxide substance of BT-4 was effective for As (V). However, less than 70% of As (III) was removed in 24 h using BT-4, whereas 80% was removed using MnBT-4. Although raw BT-4 had a moderate capacity to adsorb As (III), Mn-modified BT-4, MnBT-4, had a higher As (III) removal efficiency. This work met the goal of developing an adsorbent with an oxidative function and many adsorption sites for arsenic removal.

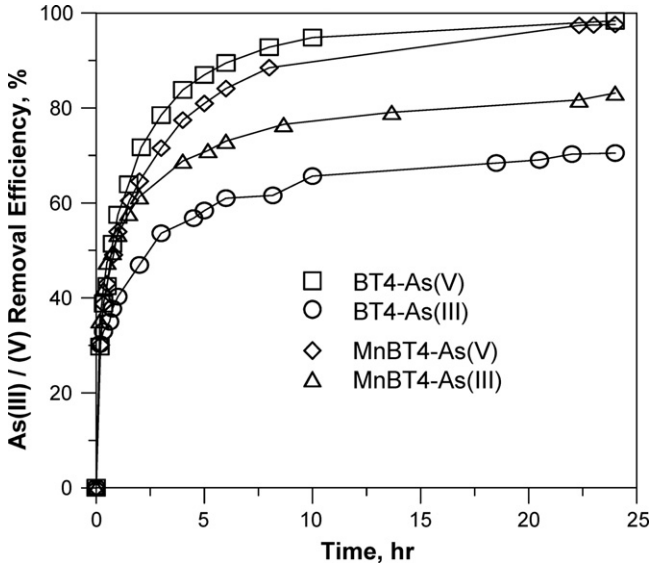

Fig. 8. As (III)/(V) adsorption efficiency of BT4 and MnBT-4 (adsorbent dosage = 2.5 g, initial [As] = 70 ppm, pH = 3).

4. Conclusions

Based on the concept of an Mn–Fe binary oxide for arsenic removal, an MnBT-4 adsorbent was developed. The $KMnO_4$ could be immobilized on BT-4 in a fluidized bed reactor (FBR). The trace Mn species that was trapped on MnBT-4 using the hydraulic system in FBR acted as a reductant, while the BT-4 substrate had a high surface area ($229\ m^2\ g^{-1}$) for the adsorption of arsenic ions. A Fe/Mn dosage ratio of less than four was found to yield highly efficient Mn immobilization. However, Mn compounds were immobilized without the introduction of ferrous ions to the FBR, implying that the Fe (II) pre-existed in BT-4. The adsorption isotherm that was fitted using the Langmuir model suggests that MnBT-4 has a high adsorption capacity, $27.4\ mg\ g^{-1}$, for As (III). MnBT-4 has a higher As (III) removal efficiency of over 80% than BT-4 which has a removal efficiency of 65%. Millimeter-scale MnBT-4 is more effective in solid–liquid separation than nano-scale coprecipitates of Mn and Fe salts in the literature. Also, sustainability factors make MnBT-4 an attractive adsorbent for removing aqueous As (III).

References

[1] J. van der Geer, J.A.J. Hanraads, R.A. Lupton, The art of writing a scientific article, J. Sci. Commun. 163 (2000) 51–59.
[2] P.L. Smedley, D.G. Kinniburgh, A review of the source, behavior and distribution of arsenic in natural waters, Appl. Geochem. 17 (2002) 517–568.
[3] F.W. Pontius, G.K. Brown, J.C. Chien, Health implications of arsenic in drinking water, J. Am. Water Works Assoc. 86 (1994) 52–63.
[4] Y.F. Pan, C.T. Chiou, T.F. Lin, Adsorption of arsenic (V) by iron-oxide-coated diatomite (IOCD), Environ. Sci. Pollut. Res. 17 (2010) 1401–1410.
[5] B. Pakzadeh, J.R. Batista, Surface complexation modeling of the removal of arsenic from ion-exchange waste brines with ferric chloride, J. Hazard. Mater. 188 (2011) 399–407.
[6] W. Tongamp, Y. Takasaki, A. Shibayama, Precipitation of arsenic as Na3AsS4 from Cu3AsS4–NaHS–NaOH leach solutions, Hydrometallurgy 105 (2010) 42–46.
[7] N. Balasubramaniana, T. Kojimab, C. Srinivasakannan, Arsenic removal through electrocoagulation: kinetic and statistical modeling, Chem. Eng. J. 155 (2009) 76–82.
[8] M.B. Baskan, A. Pala, A statistical experiment design approach for arsenic removal by coagulation process using aluminum sulfate, Desalination 254 (2010) 42–48.
[9] R.S. Harisha, K.M. Hosamani, R.S. Keri, S.K. Nataraj, T.M. Aminabhavi, Arsenic removal from drinking water using thin film composite nanofiltration membrane, Desalination 252 (2010) 75–80.
[10] M. Sen, A. Manna, P. Pal, Removal of arsenic from contaminated groundwater by membrane-integrated hybrid treatment system, J. Membrane Sci. 354 (2010) 108–113.
[11] B.K.C. Chan, A.W.L. Dudeney, Reverse osmosis removal of arsenic residues from bioleaching of refractory gold concentrates, Miner. Eng. 21 (2008) 272–278.
[12] J.S. Zhang, R.S. Stanforth, S.O. Pehkonen, Effect of replacing a hydroxyl group with a methyl group on arsenic (V) species adsorption on goethite (α-FeOOH), J. Colloid Interface Sci. 306 (2007) 16–21.
[13] Y. Jeong, F. Maohong, J.V. Leeuwen, J.F. Belczyk, Effect of competing solutes on arsenic(V) adsorption using iron and aluminum oxides, J. Environ. Sci. 19 (2007) 910–919.
[14] W. Yang, A.T. Kan, W. Chen, M.B. Tomson, pH-dependent effect of zinc on arsenic adsorption to magnetite nanoparticles, Water Res. 44 (2010) 5693–5701.
[15] Y. Tang, J. Wang, N. Gao, Characteristics and model studies for fluoride and arsenic adsorption on goethite, J. Environ. Sci. 22 (11) (2010) 1689–1694.
[16] G.S. Zhang, J.H. Qu, H.J. Liu, R.P. Liu, G.T. Li, Removal mechanism of As(III) by a novel Fe–Mn binary oxide adsorbent: oxidation and sorption, Environ. Sci. Technol. 41 (2007) 4613–4619.
[17] J.N. Moore, J.R. Walker, T.H. Hayes, Reaction scheme for the oxidation of As(III) to As(V) by birnessite, Clays Clay Miner. 38 (1990) 549–555.
[18] W. Driehaus, R. Seith, M. Jekel, Oxidation of arsenate (III) with manganese oxides in water treatment, Water Res. 29 (1995) 297–305.
[19] H.W. Nesbitt, G.W. Canning, G.M. Bancroft, XPS study of reductive dissolution of 7 Å-birnessite by H_3AsO_3 with constraints on reaction mechanism, Geochim. Cosmochim. Acta 62 (1998) 2097–2110.
[20] V. Lenoble, C. Laclautre, B. Serpaud, V. Deluchat, J.C. Bollinger, As(V) retention and As(III) simultaneous oxidation and removal on a MnO_2-loaded polystyrene resin, Sci. Total Environ. 326 (2004) 197–207.
[21] G. Zhang, J. Qu, H. Liu, R. Liu, R. Wu, Preparation and evaluation of a novel Fe–Mn binary oxide adsorbent for effective arsenite removal, Water Res. 41 (2007) 1921–1928.
[22] Y.H. Huang, Y.J. Shih, C.C. Chang, Adsorption of fluoride by waste iron oxide: the effects of solution pH, major coexisting anions, and adsorbent calcination temperature, J. Hazard. Mater. 186 (2011) 1355–1359.
[23] Y.H. Huang, C.L. Hsueh, H.P. Cheng, L.C. Su, C.Y. Chen, Thermodynamics and kinetics of adsorption of Cu(II) onto waste iron oxide, J. Hazard. Mater. 144 (1–2) (2007) 406–411.
[24] Y.H. Huang, C.L. Hsueh, C.P. Huang, L.C. Su, C.Y. Chen, Adsorption thermodynamic and kinetic studies of Pb(II) removal from water onto a versatile Al_2O_3-supported iron oxide, Sep. Purif. Technol. 55 (1) (2007) 23–29.
[25] Y.H. Huang, Y.J. Shih, C.C. Chang, S.H. Chuang, A comparative study of phosphate removal technologies using adsorption and fluidized bed crystallization process, Desalin. Water Treat. 32 (2011) 351–356.
[26] D. Postma, C.A.J. Appelo, Reduction of Mn-oxides by ferrous iron in a flow system: column experiment and reactive transport modeling, Geochim. Cosmochim. Acta 64 (2000) 1237–1247.
[27] X. Guana, J. Ma, H. Dong, L. Jiang, Removal of arsenic from water: effect of calcium ions on As(III) removal in the $KMnO_4$–Fe(II) process, Water Res. 43 (2009) 5119–5128.
[28] H.L. Lien, R.T. Wilkin, High-level arsenite removal from groundwater by zero-valent iron, Chemosphere 59 (2005) 377–386.
[29] P. Lakshmipathiraj, B.R.V. Narasimhan, S. Prabhakar, G.B. Raju, Adsorption studies of arsenic on Mn-substituted iron oxyhydroxide, J. Colloid Interface Sci. 304 (2006) 317–322.
[30] B. Prasad, C. Ghosh, A. Chakraborty, N. Bandyopadhyay, R.K. Ray, Adsorption of arsenite (As3+) on nano-sized Fe_2O_3 waste powder from the steel industry, Desalination 274 (2011) 105–112.
[31] K. Simeonidis, Th. Gkinis, S. Tresintsi, C. Martinez-Boubeta, G. Vourlias, I. Tsiaoussis, G. Stavropoulos, M. Mitrakas, M. Angelakeris, Magnetic separation of hematite-coated Fe_3O_4 particles used as arsenic adsorbents, Chem. Eng. J. 168 (2011) 1008–1015.
[32] S. Paikaray, J. Göttlicher, S. Peiffer, Removal of As(III) from acidic waters using schwertmannite: surface speciation and effect of synthesis pathway, Chem. Geol. 283 (2011) 134–142.
[33] A. Maiti, S. DasGupta, J.K. Basu, S. De, Adsorption of arsenite using natural laterite as adsorbent, Sep. Purif. Technol. 55 (2007) 350–359.
[34] J. Hao, M.J. Han, X. Meng, Preparation and evaluation of thiol-functionalized activated alumina for arsenite removal from water, J. Hazard. Mater. 167 (2009) 1215–1221.
[35] K. Grover, S. Komarneni, H. Katsuki, Uptake of arsenite by synthetic layered double hydroxides, Water Res. 43 (2009) 3884–3890.
[36] C.A. Martinson, K.J. Reddy, Adsorption of arsenic(III) and arsenic(V) by cupric oxide nanoparticles, J. Colloid Interface Sci. 336 (2009) 406–411.
[37] S. Chakraborty, M. Wolthers, D. Chatterjee, L. Charlet, Adsorption of arsenite and arsenate onto muscovite and biotite mica, J. Colloid Inter. Sci. 309 (2007) 392–401.
[38] H. Amiri, N. Jaafarzadeh, M. Ahmadi, S.S. Martínez, Application of LECA modified with Fenton in arsenite and arsenate removal as an adsorbent, Desalination 272 (2011) 212–217.